POLQ promotes tumor progression and immunosuppression via ATM-P53 signaling in endometrial cancer

NINGNING ZHU[1*], JUANJUAN WANG[1*], XIAOLI ZHANG[2*], KAI TANG[2], LEI GONG[3] and YI HU[1,4]

[1]School of Medicine, Nankai University, Tianjin 300071, P.R. China; [2]Department of Pediatrics, Affiliated Taihe Hospital of Hubei University of Medicine, Shiyan, Hubei 442000, P.R. China; [3]Department of Esophageal Cancer, Tianjin Medical University Cancer Institute and Hospital, National Clinical Research Center for Cancer, Tianjin 300060, P.R. China; [4]Department of Oncology, The Fifth Medical Center of People's Liberation Army General Hospital, Beijing 100039, P.R. China

Received November 4, 2025; Accepted February 11, 2026

DOI: 10.3892/or.2026.9097

Abstract. Endometrial cancer (EC) is a one of the most prevalent gynecological malignancies worldwide; however, the molecular mechanisms driving its progression remain insufficiently understood. In the present study, DNA polymerase θ (POLQ), which is implicated in multiple types of cancer, was comprehensively investigated in EC using data from The Cancer Genome Atlas and TNMplot datasets, with further validation in an independent patient cohort. POLQ expression was markedly upregulated in EC tissues and was associated with reduced 15-year overall survival. Increased POLQ levels were also associated with higher Ki67 proliferation indices, distinct patterns of T-cell infiltration and enhanced programmed death-ligand 1 (PD-L1) expression. Gene Set Enrichment Analysis revealed that POLQ expression was associated with pathways involved in cell proliferation, cell cycle regulation and DNA damage repair. Mechanistic studies based on POLQ knockdown in EC cells were conducted *in vitro* using small interfering RNA-mediated gene silencing, followed by functional assays including cell proliferation assay, flow cytometric cell cycle analysis, apoptosis assay, migration and invasion assays, and western blot analysis to detect the expression of key proteins involved in ATM/P53 signaling and epithelial-mesenchymal transition (EMT) regulation. These experiments further demonstrated that POLQ may accelerate EC progression via two complementary mechanisms: i) Activation of ataxia-telangiectasia mutated/P53 signaling to facilitate cell cycle checkpoint bypass; and ii) induction of EMT via cadherin switching. Collectively, these findings established POLQ as a robust prognostic biomarker and a promising therapeutic target in EC.

Correspondence to: Professor Yi Hu, Department of Oncology, The Fifth Medical Center of People's Liberation Army General Hospital, 100 Xisihuan Middle Road, Fengtai, Beijing 100039, P.R. China
E-mail: huyi301zlxb@sina.com

Professor Lei Gong, Department of Esophageal Cancer, Tianjin Medical University Cancer Institute and Hospital, National Clinical Research Center for Cancer, 1 Tiyuanbeidao Huanhuxi Road, Hexi, Tianjin 300060, P.R. China
E-mail: leigong@tmu.edu.cn

*Contributed equally

Key words: polymerase θ, endometrial cancer, tumorigenesis, cell cycle

Introduction

Endometrial cancer (EC) is the fifth most commonly diagnosed malignancy worldwide and remains one of the most lethal types of gynecological cancer (1). Notably, ~75% of patients are diagnosed at an early stage (FIGO stage I-II), with a favorable overall 5-year survival rate of ~80%. By contrast, patients diagnosed at an advanced stage (FIGO stage III) exhibit markedly poorer outcomes, with reported 5-year survival rates ranging between 25 and 60% (2). Despite advances in therapeutic approaches, including surgery, chemotherapy, radiotherapy and hormonal therapy, the incidence and mortality of EC have continued to increase (3). These trends highlight an urgent need to elucidate the molecular mechanisms underlying EC progression, and to identify novel biomarkers and therapeutic targets to improve prognostic assessment and clinical management.

DNA polymerase θ (POLQ, also known as Polθ), encoded by the POLQ gene, is a key mediator of microhomology-mediated end joining (MMEJ), a DNA double-strand break (DSB) repair pathway that mediates the ligation of excised 3' DNA ends using microhomologous sequences (4,5). Structurally, POLQ consists of a C-terminal DNA polymerase domain, an N-terminal helicase-like domain with DNA-dependent ATPase activity, and a non-conserved central domain (6). During the S phase of the cell cycle, MMEJ directly competes with homologous recombination (HR) for DNA end binding, thus serving a critical role in DNA damage repair (7,8). Tumors with HR deficiency are particularly dependent on POLQ-mediated repair mechanisms (9). Aberrant POLQ expression has been reported across multiple malignancies, including colorectal (10), lung (11) and breast cancer (12,13), where its increased expression is consistently associated with unfavorable clinical outcomes (14-16). Beyond its established functions in DNA replication, cell cycle

regulation and genome stability, POLQ has also been implicated in immune regulation (17), cancer stemness and ferroptosis (12). However, to the best of our knowledge, the molecular mechanisms and prognostic importance of POLQ in EC have not been previously investigated.

Therefore, the current study aimed to systematically analyze POLQ expression in EC, and to investigate its association with the immune checkpoint protein programmed death-ligand 1 (PD-L1) using data from The Cancer Genome Atlas (TCGA), with validation in EC patient specimens. Furthermore, the functional effects of POLQ on EC cell proliferation and tumor progression, as well as the underlying molecular mechanisms, were further investigated through *in vitro* experiments. Collectively, these findings may provide novel insights into the oncogenic role of POLQ in EC, and support its potential value as both a prognostic biomarker and a therapeutic target.

Materials and methods

Assessment of POLQ expression in EC using publicly available databases. A total of two publicly available databases were utilized: TCGA Uterine Corpus Endometrial Carcinoma (TCGA-UCEC) project via the Genomic Data Commons portal (https://portal.gdc.cancer.gov/) and the TNMplot online database (https://tnmplot.com/). Transcriptomic profiles of 554 EC tissues and 35 adjacent non-tumor endometrial tissues were retrieved from TCGA-UCEC. In parallel, expression data from 469 EC tissues and 315 normal endometrial tissues from healthy controls were retrieved from the TNMplot database, which integrates RNA-sequencing (RNA-seq) data from TCGA, Genotype-Tissue Expression and Gene Expression Omnibus cohorts (18).

Association between POLQ expression and clinicopathological characteristics. To evaluate the association between POLQ expression and clinicopathological features, association analysis using data from TCGA-EC cohort was conducted. Patients were stratified into high- and low-expression groups based on the median POLQ expression levels (n=277/group). RNA-seq data and the corresponding clinical information were retrieved from TCGA. Clinicopathological variables included age, body mass index (BMI), histological subtype, tumor grade, clinical stage and survival status. The prognostic significance of POLQ expression was assessed using overall survival (OS), disease-specific survival (DSS) and progression-free interval (PFI). Survival curves were generated using the Kaplan-Meier method and compared using the log-rank test. Furthermore, univariate Cox proportional hazards regression and multivariate Cox regression analyses were performed to determine whether POLQ expression was independently associated with survival outcomes in TCGA-EC cohort. All statistical analyses were conducted using R software (version 4.3.1; R Foundation for Statistical Computing; https://www.r-project.org/). Survival analyses were performed using the 'survival' package (version 3.8-6; https://cran.r-project.org/package=survival) and 'survminer' package (version 0.5.1; https://cran.r-project.org/package=survminer) in R.

Immune infiltration and gene set enrichment analysis (GSEA). Immune infiltration analysis and GSEA were performed using TCGA-UCEC cohort. The Estimation of Stromal and Immune Cells in Malignant Tumor Tissues using Expression Data (ESTIMATE) algorithm (19) was employed to assess the relative abundance of stromal and immune cells within tumor samples based on gene expression profiles. Immune infiltration analyses, including the calculation of stromal, immune and ESTIMATE scores, were carried out using the 'estimate' R package (version 1.0.13; https://r-forge.r-project.org/projects/estimate/) in R software (version 4.3.1), based on transcriptomic data from TCGA-UCEC cohort. Briefly, the ESTIMATE algorithm calculates stromal and immune scores based on single-sample GSEA of predefined stromal- and immune-related gene signatures, and the ESTIMATE score is derived from the combination of the stromal and immune scores. Additionally, the relative abundance of specific immune cell populations was assessed using the 'GSVA' R package (version 1.46.0) (20-22). In addition, GSEA, including Hallmark pathway analysis, and Kyoto Encyclopedia of Genes and Genomes (KEGG) pathway enrichment analyses were performed using R software (version 4.3.1). GSEA was conducted using the 'clusterProfiler' package (version 4.6.2; https://bioconductor.org/packages/clusterProfiler/), and gene sets were obtained from the Molecular Signatures Database (MSigDB, version 7.5.1; https://www.gsea-msigdb.org/gsea/msigdb), including the Hallmark gene set collection. KEGG pathway enrichment analysis was also performed using 'clusterProfiler'. Pathways with a false discovery rate <0.25 were considered significantly enriched. Spearman's correlation coefficients were calculated to evaluate the associations between POLQ expression levels and pathway enrichment scores, with a significance threshold set at rs>0.5 and P<0.05.

Differential expression and Gene Ontology (GO) enrichment analyses. Differential expression analysis between the POLQ-high and POLQ-low groups was performed using the 'limma' R package (version 3.54.0; https://bioconductor.org/packages/limma/) in R software (version 4.3.1). RNA-seq data from TCGA-UCEC cohort were analyzed, and patients were stratified into POLQ-high and POLQ-low groups based on the median expression level of POLQ. Linear models were fitted using the limma framework, and empirical Bayes moderation was applied. Genes with P<0.05 and |log2FC |>1.5 were considered significantly differentially expressed. Volcano plots were generated using the 'ggplot2' R package (version 3.4.2; https://cran.r-project.org/package=ggplot2), with significance thresholds set at |log2FC|>1.5 and P<0.05. GO enrichment analysis of the identified DEGs was conducted using the 'clusterProfiler' R package (version 4.6.2). Enriched GO terms in the Biological Process categories were identified. GO terms with P<0.05 were considered significantly enriched.

Clinical specimens and immunohistochemistry (IHC). A total of 113 formalin-fixed paraffin-embedded (FFPE) tissue specimens, including 78 EC tissues and 35 paired adjacent non-cancerous endometrial tissues, were collected from Taihe Hospital (Shiyan, China) between July 2020 and October 2023. The tissues were fixed in 10% neutral buffered formalin at room temperature (20-25˚C) for 24 h prior to routine dehydration and paraffin embedding. All patients with EC were female, with a median age of 59 years (range, 41-72 years). All diagnoses were confirmed by senior pathologists, and none of

the patients had received preoperative radiotherapy or chemotherapy. FFPE tissue blocks were cut into 3-μm sections, which were deparaffinized in xylene, rehydrated through graded ethanol and subjected to heat-induced antigen retrieval using EDTA buffer (pH 9.0) at 95-100˚C for 15 min. Endogenous peroxidase activity was blocked following incubation with 3% hydrogen peroxide for 10 min at room temperature. After blocking with QuickBlock™ Blocking Buffer for Immunol Staining (cat. no. P0260; Beyotime Biotechnology) at room temperature for 15 min to reduce non-specific binding, the sections were incubated at 4˚C overnight with primary antibodies against POLQ, Ki67 and PD-L1 (Table SI), followed by incubation with horseradish peroxidase (HRP)-conjugated secondary antibodies (ready-to-use; cat. no. PV-6000; Beijing Zhongshan Jinqiao Biotechnology Co., Ltd.) at room temperature for 30 min. Immunoreactivity was visualized using DAB as the chromogen and cell nuclei were counterstained with hematoxylin at room temperature for 1 min. POLQ expression levels were semi-quantitatively scored based on staining quantity (0-4) and intensity (0-3), with final overall scores calculated as quantity x intensity (range, 0-12). Ki67 positive expression was quantified as the percentage of $Ki67^+$ cells at x200 magnification. PD-L1 IHC was carried out using a PD-L1 antibody (clone no. 22C3; ready-to-use; cat. no. SK006; Dako; Agilent Technologies, Inc.), which was used to incubate the sections at 4˚C overnight. Detection was carried out using the EnVision™ FLEX HRP detection kit (cat. no. K8000; Dako; Agilent Technologies, Inc.), which includes an HRP-conjugated secondary antibody polymer, according to the manufacturer's instructions. PD-L1 expression was evaluated using a semi-quantitative IHC scoring system. Staining intensity was scored as 0 (negative), 1 (weak), 2 (moderate) or 3 (strong), and the proportion of positive tumor cells was scored from 0 to 5 according to the percentage of positive cells. The final IHC score was calculated as the sum of the intensity and proportion scores, yielding a total score ranging from 0 to 8 (23). All slides were independently evaluated by at least two experienced pathologists using a bright-field light microscope (Olympus Corporation).

Cell culture and transfection. HEC-1-B and Ishikawa cells were obtained from The Cell Bank of Type Culture Collection of The Chinese Academy of Sciences and cultured in RPMI-1640 medium (Gibco; Thermo Fisher Scientific, Inc.) supplemented with 10% fetal bovine serum (FBS; Gibco; Thermo Fisher Scientific, Inc.). Cells were maintained at 37˚C in a humidified incubator with 5% CO_2. Once they had reached ~90% confluence, the cells were passaged and were then seeded in 6-well plates for further experiments. Upon reaching ~30% confluence, the cells were transfected with small interfering (si)RNAs targeting POLQ (si-POLQ#1 and si-POLQ#2) or the corresponding negative control siRNA (si-NC)(all synthesized by Sangon Biotech Co., Ltd.), at a final concentration of 50 nM using GenMute™ siRNA Transfection Reagent (cat. no. SL100568; SignaGen Laboratories), according to the manufacturer's instructions. The culture medium was replaced at 6 h post-transfection. Transfection was performed at 37˚C in a humidified incubator with 5% CO_2. To detect the mRNA expression levels of target genes, cells were harvested at 24 h post-transfection, whereas protein expression levels were assessed 48 h post-transfection. All subsequent functional assays were performed 48 h after transfection unless otherwise specified. All experiments were performed in triplicate. The siRNA sequences used are listed in Table SII.

Reverse transcription-quantitative PCR (RT-qPCR). Total RNA was extracted from the transfected cells using the RNAeasy™ Animal RNA Extraction Kit (cat. no. R0024; Beyotime Biotechnology), which is designed for mammalian cells, according to the manufacturer's instructions. cDNA was then synthesized using the Evomak-Mlo Reverse Transcription Kit (cat. no. AG11705; Hunan Accurate Bio-Medical Technology Co., Ltd.) according to the manufacturer's protocol. qPCR was performed using TB Green® Premix Ex Taq™ II (Tli RNaseH Plus) (cat. no. RR820A; Takara Bio, Inc.) according to the manufacturer's instructions. The thermocycling conditions were as follows: 95˚C for 30 sec, followed by 40 cycles at 95˚C for 5 sec and 60˚C for 30 sec. A melt curve analysis was performed to confirm amplification specificity. Relative mRNA expression levels were calculated using the $2^{-\Delta\Delta Cq}$ method (24). The primer sequences used are listed in Table SII.

Western blot analysis. Transfected cells were lysed on ice for 30 min using Western and IP Cell Lysis Buffer (cat. no. P0037; Beyotime Biotechnology) and cell lysates were centrifuged at 12,000 x g for 15 min at 4˚C and the supernatants were collected for subsequent analysis. Protein concentrations were calculated using a BCA assay (cat. no. P0012S; Beyotime Biotechnology). Subsequently, equal amounts of protein samples (30 μg per lane) were mixed with loading buffer, separated by SDS-PAGE using different percentages of polyacrylamide gels according to the molecular weights of the target proteins (6-15%), and transferred onto PVDF membranes. After blocking with 5% skimmed milk for 1 h at room temperature, the membranes were incubated overnight at 4˚C with primary antibodies against the target proteins listed in Table SII. After washing with TBS-0.1% Tween-20 three times, the membranes were incubated with HRP-conjugated goat anti-rabbit IgG (H+L) (1:10,000; cat. no. SA00001-2; Wuhan Sanying Biotechnology) or HRP-conjugated goat anti-mouse IgG (H+L) (1:10,000; cat. no. SA00001-1; Wuhan Sanying Biotechnology) for 1 h at room temperature. The protein bands were then visualized using an enhanced chemiluminescence substrate (cat. no. MA0187; Dalian Meilun Biology Technology Co., Ltd.) on a Bio-Rad gel imaging system (Bio-Rad Laboratories, Inc.). The detailed information of all primary antibodies used for western blot analysis, including the antibody sources, catalog numbers and dilutions, is provided in Table SIII.

Cell Counting Kit 8 (CCK-8) assay. Cells were collected and, following transfection for 48 h, were counted and seeded in 96-well plates at a density of 2,000 cells/well. Cell viability was then assessed at 24, 48, 72 and 96 h after seeding. Following incubation for the indicated time points, each well was supplemented with 10 μl CCK-8 reagent (cat. no. BS350A; Biosharp Life Sciences), followed by incubation for an additional 1 h at 37˚C. The optical density in each well was then measured at an absorbance of 450 nm using a microplate reader.

Colony formation assay. Transfected HEC-1-B and Ishikawa cells were digested, counted using a hemocytometer (Neubauer chamber) and seeded into 6-well plates at a density of 500 cells/well, with three replicates per group. The cells were incubated for 7-14 days depending on the growth rate of the cell lines, until visible colonies (≥50 cells/colony) had formed. Subsequently, the plates were washed with PBS and the colonies were fixed in 100% methanol at room temperature for 15 min. After fixation, the colonies were stained with 0.5% crystal violet solution (MilliporeSigma) at room temperature for 20 min. Colonies were counted manually under a bright-field light microscope (CX43; Olympus Corporation) and representative images were captured using a smartphone camera attached to the bright-field light microscope.

EdU proliferation assay. Transfected HEC-1-B and Ishikawa cells were trypsinized, counted and seeded in 96-well plates at a density of $2x10^4$ cells/well. The cells were then incubated with EdU (final concentration: 10 μM; Beyotime Biotechnology) at 37˚C for 2 h. Subsequently, cells were fixed with 4% paraformaldehyde at room temperature for 15 min, followed by permeabilization with 0.3% Triton X-100 at room temperature for 10 min, according to the manufacturer's instructions. EdU incorporation was detected using the Click reaction solution, and cell nuclei were counterstained with Hoechst 33342, according to the BeyoClick™ EdU-594 Cell Proliferation Assay Kit protocol (cat. no. C0078S; Beyotime Biotechnology). Fluorescence images were captured under a fluorescence microscope. EdU-positive proliferating cells displayed red fluorescence, whereas total nuclei were visualized by blue fluorescence. The proliferation rate was calculated as the ratio of EdU-positive cells to the total number of cells.

Transwell assay. For the Transwell migration assays, transfected HEC-1-B and Ishikawa cells were digested, washed twice with serum-free RPMI-1640 medium, and resuspended at a density of $1.5x10^5$ cells/well in 24-well Transwell plates (pore size, 8 μm). Cell suspensions were seeded into the upper chamber of Transwell inserts in serum-free medium, whereas 600 μl RPMI-1640 medium containing 10% FBS was added to the lower chamber as a chemoattractant. Following incubation at 37˚C for 24 h, non-migrated cells on the upper surface of the membrane were gently removed and the inserts were washed twice with PBS. Migrated cells on the lower surface were fixed with 4% paraformaldehyde for 30 min at 25˚C and stained with 0.1% crystal violet for 20 min at 25˚C. Excess stain was then removed by washing three times with double-distilled water, and, after drying, migrated cells were visualized and images were using an inverted light microscope (Olympus Corporation).

For the invasion assays, Transwell inserts were precoated with Matrigel (cat. no. 356234; Corning, Inc.). Briefly, pre-melted Matrigel was diluted and added to the upper surface of the Transwell chamber, followed by incubation at 37˚C overnight to allow polymerization. Subsequently, the cells were harvested and resuspended at a density of $7.5x10^5$/well. The subsequent procedures were performed as described for the Transwell migration assays.

Wound healing assay. For wound healing assays, transfected HEC-1-B and Ishikawa cells were seeded into 6-well plates and cultured until they reached ~90% confluence. Subsequently, a straight scratch was created in each well using a 200-μl pipette tip. The detached cells were removed after washing twice with PBS and the cells were then cultured in serum-free medium. Images of the wound area were captured immediately after scratching (0 h) under an inverted phase-contrast light microscope (magnification, x10). Following incubation at 37˚C for 24 h in a humified atmosphere with 5% CO_2, images of the same wound areas were captured. The wound area was semi-quantified using ImageJ software (version 1.53a; National Institutes of Health), and the cell migration rate was calculated using the following formula: Migration rate (%)=[(wound area at 0 h-wound area at 24 h)/wound area at 0 h] x100.

Apoptosis assessment by flow cytometry. Following transfection, the culture supernatants were collected and adherent cells were detached using 0.25% trypsin without EDTA at 37˚C for 3 min; digestion was terminated by the addition of complete medium. The cells were then pooled with the collected supernatants and centrifuged at 300 x g for 5 min at 4˚C for further analysis. Both suspended and adherent cells were pooled, washed twice with PBS and resuspended. A total of $1x10^4$ cells/well were resuspended in 100 μl binding buffer and incubated with 5 μl Annexin V-FITC and 2 μl propidium iodide (PI) for 15 min at room temperature in the dark, according to the manufacturer's instructions (Annexin V-FITC/PI Apoptosis Detection Kit; cat. no. 556547; BD Biosciences). Staining was terminated by adding 400 μl binding buffer, and the cell apoptosis rate was subsequently analyzed by flow cytometry (FACSCalibur; BD Biosciences) using FlowJo 7.6 software (BD Biosciences).

Cell cycle assay. Transfected cells were seeded into 6-well plates and harvested when they reached ~80% confluence. The cells were then digested with 0.25% trypsin without EDTA, washed with PBS and resuspended in 300 μl cell cycle staining solution (Cell Cycle and Apoptosis Analysis Kit; cat. no. CCS012; MultiSciences Biotech Co., Ltd.) containing PI and RNase A. Following incubation at 37˚C for 30 min in the dark, cell cycle distribution was analyzed using a BD FACSCanto II flow cytometer (BD Biosciences). The proportion of cells in each phase of the cell cycle was quantified using FlowJo 7.6 software.

Statistical analysis. All statistical analyses were performed using GraphPad Prism 8.0 (Dotmatics). Data are presented as the mean ± standard deviation, and all *in vitro* experiments were conducted in triplicate. For normally distributed continuous variables, paired or unpaired Student's t-tests were used to compare the differences between two groups. Non-normally distributed data were analyzed using the Wilcoxon rank-sum test. Comparisons among multiple groups were carried out using one-way ANOVA followed by Bonferroni post hoc test. Categorical variables were analyzed using the χ^2 test, as all expected frequencies were ≥5. Correlations were assessed using Spearman's rank correlation coefficient. Survival analyses were performed using the Kaplan-Meier method and compared using the log-rank test.

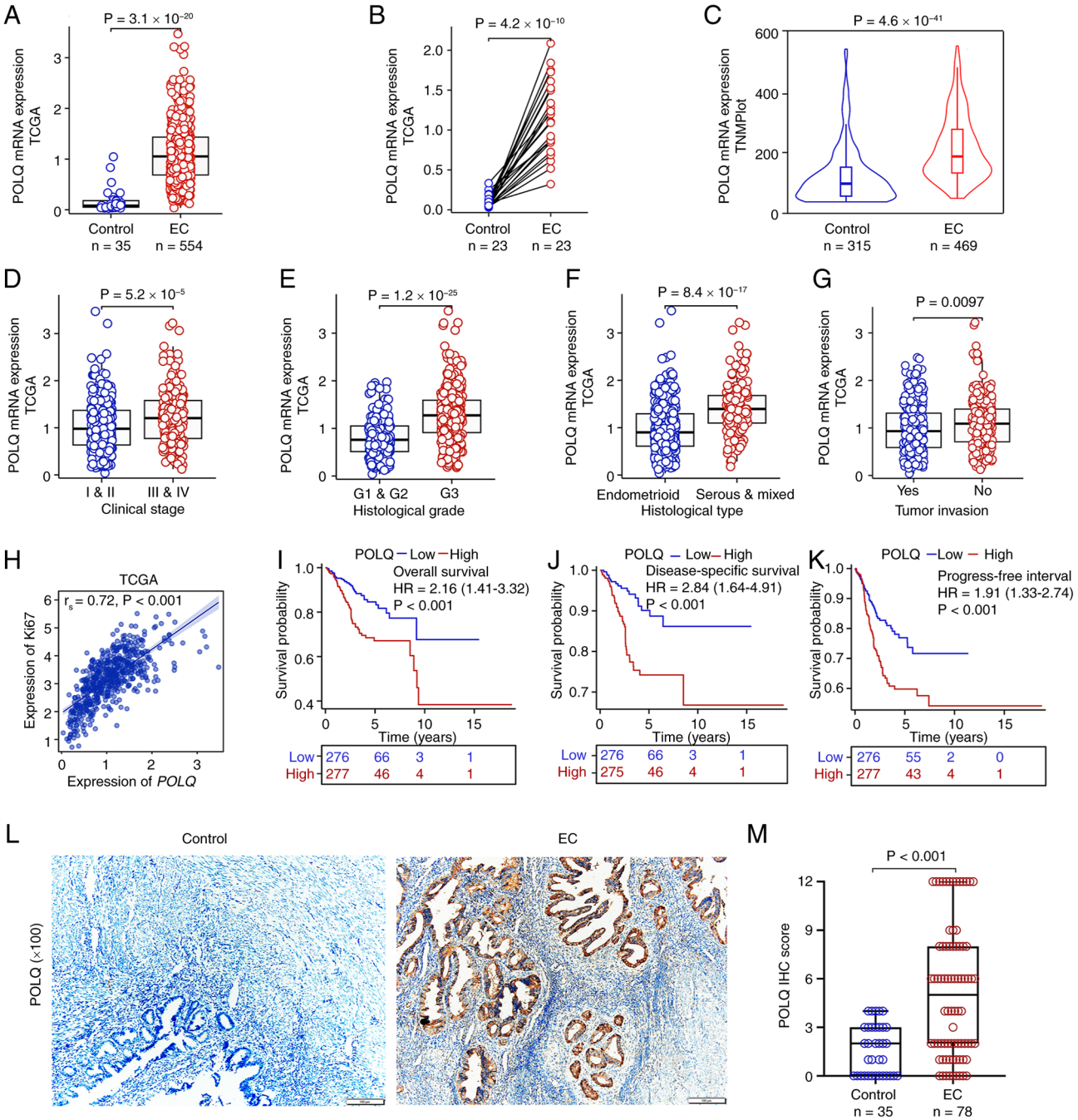

Figure 1. Aberrant expression of POLQ in EC. Expression levels of POLQ in EC tissues compared with control tissues based on (A) unpaired TCGA, (B) paired TCGA and (C) TNMplot datasets. Association between POLQ expression and clinicopathological features in EC, including (D) clinical stage, (E) histological grading, (F) histological type and (G) tumor invasion. (H) Correlation analysis of POLQ expression and Ki67 expression based on TCGA-EC data. Prognostic analysis of POLQ expression in EC based on TCGA data, including (I) overall survival, (J) disease-specific survival and (K) progression-free interval. (L) IHC images of POLQ in EC (n=78) and adjacent non-cancerous control tissues (n=35); x100 magnification. (M) IHC score of POLQ in EC and adjacent non-cancerous control tissues. EC, endometrial cancer; IHC, immunohistochemistry; POLQ, DNA polymerase θ; TCGA, The Cancer Genome Atlas.

Two-tailed P<0.05 was considered to indicate a statistically significant difference.

Results

POLQ is upregulated in EC, and is associated with adverse clinicopathological features and a poor prognosis. Comprehensive bioinformatics analyses using multiple publicly available tumor databases, including TNMplot and TCGA-EC cohort, demonstrated that POLQ mRNA expression was significantly increased in EC tissues compared with that in adjacent normal tissues (Fig. 1A-C). Clinicopathological analyses further revealed that high POLQ expression was significantly associated with patient age, histological subtype and grade, and clinical stage, whereas no significant associations were observed with BMI or residual tumor status (Table SIV). Notably, POLQ expression was markedly increased in patients with advanced clinical stage EC (Fig. 1D), a higher histological grade (Fig. 1E), a more aggressive histological subtype (Fig. 1F) and tumor invasion (Fig. 1G), compared with

their respective control groups. Correlation analysis based on TCGA-EC data further showed a positive association between POLQ expression and the proliferation marker Ki67 (Fig. 1H), suggesting a potential role for POLQ in promoting tumor cell proliferation. Additionally, survival analyses further revealed that high POLQ expression was significantly associated with unfavorable OS (Fig. 1I), DSS (Fig. 1J) and PFI (Fig. 1K). Univariate Cox regression analysis demonstrated that POLQ expression was significantly associated with overall survival in patients with EC. However, this association was not maintained in the multivariate Cox regression analysis (P=0.393), indicating that POLQ expression was not an independent prognostic factor (Table SV). To further validate the aforementioned findings at the protein level, IHC analysis was performed on tissue microarrays comprising 78 EC specimens and 35 paired adjacent non-cancerous endometrial tissues. POLQ expression was semi-quantitatively evaluated based on both staining intensity and quantity. Consistent with the transcriptomic data, POLQ protein expression levels were markedly elevated in EC tissues compared with those in adjacent non-cancerous controls (Fig. 1L and M), thus supporting the oncogenic role of POLQ in EC. Taken together, these findings suggest that POLQ is upregulated in EC, and is associated with aggressive clinicopathological features and poor prognosis, potentially contributing to tumor progression, although it does not serve as an independent prognostic factor.

POLQ expression is associated with an immunosuppressive tumor microenvironment in EC. To further elucidate the biological role of POLQ in EC, its association with the tumor immune microenvironment was evaluated using TCGA data. GSEA suggested that aberrant POLQ expression could affect the infiltration of multiple immune cell populations, with significantly reduced infiltration of T cells and natural killer (NK) cells in the high POLQ expression group compared with the low POLQ expression group (Fig. 2A). Consistently, analysis using the ESTIMATE algorithm revealed that stromal, immune and composite ESTIMATE scores were significantly decreased in EC samples with high POLQ expression (Fig. 2B). Furthermore, correlation analyses demonstrated that POLQ expression was weakly negatively correlated with $CD8^+$ T-cell infiltration, and was also negatively correlated with the infiltration of NK cells and dendritic cells, while showing a positive correlation with T helper 2 cells (Fig. 2C). Notably, POLQ expression exhibited a weak but statistically significant positive correlation with immune checkpoint-related molecules, particularly with CD274 (PD-L1; Fig. 2D). Consistent with these findings, the expression levels of CD274, lymphocyte activation gene 3, programmed cell death 1 ligand 2, and T cell immunoreceptor with Ig and ITIM domains were significantly increased in POLQ-high EC samples compared with in POLQ-low samples (Fig. 2E). Further correlation analyses confirmed a weak but statistically significant association between POLQ and CD274 (PD-L1) expression (Fig. 2F), as well as a notable association between POLQ expression and microsatellite instability score (Fig. 2G) . Collectively, these findings suggest that elevated POLQ expression is associated with an immunosuppressive tumor microenvironment in EC, characterized by reduced cytotoxic immune cell infiltration and increased expression of immune checkpoint-related molecules.

POLQ expression is positively associated with $Ki67^+$ cells and PD-L1 expression in EC. Ki67, a well-established marker of cellular proliferation, was employed to investigate the association between POLQ expression and tumor growth in EC. In parallel, the expression levels of CD274 (PD-L1), an immune checkpoint molecule with immunosuppressive functions, were also detected. Using IHC assays, the association between POLQ expression, proliferative activity and immunosuppressive signaling was assessed in EC tissues. The results demonstrated that the proportion of $Ki67^+$ cells was significantly higher in the POLQ-high subgroup compared with that in the POLQ-low subgroup (Fig. 3A and B). Consistently, POLQ expression levels, quantified by IHC scoring, showed a significant positive correlation with the percentage of $Ki67^+$ cells (Fig. 3D). In addition, PD-L1 expression was markedly increased in POLQ-high EC tissue samples compared with that in POLQ-low tissues (Fig. 3A and C), and POLQ expression was positively associated with PD-L1 levels (Fig. 3E), thus indicating that POLQ upregulation could be involved in the establishment of an immunosuppressive tumor microenvironment in EC.

POLQ upregulation is associated with cell cycle progression and DNA repair pathways in EC. To elucidate the potential molecular mechanisms underlying the effects of POLQ on EC, GSEA and KEGG enrichment analyses were performed to identify molecular pathways associated with differential POLQ expression. GSEA revealed that EC samples with high POLQ expression were significantly enriched in pathways associated with tumor cell proliferation, DNA repair, the G_2/M cell cycle checkpoint and DNA replication (Fig. 4A). Hallmark pathway analysis further confirmed strong associations between POLQ upregulation and DNA repair [normalized enrichment score (NES)=1.84; P=0.008], as well as the G_2/M checkpoint (NES=2.14; P<0.001; Fig. 4B). Consistently, KEGG pathway analysis revealed that high POLQ expression was significantly associated with 'cell cycle' (NES=2.10; P=0.002) and 'DNA replication' (NES=1.96; P<0.001), both of which are critical drivers of tumor cell proliferation and progression (Fig. 4C). Differentially expressed genes (DEGs) between POLQ-high and POLQ-low groups are presented in Fig. 4D. Subsequent GO enrichment analysis of these DEGs further indicated that aberrant POLQ expression predominantly affected EC tumorigenesis and progression through regulation of the 'Cell Cycle, Mitotic', 'DNA Replication' and 'ATM pathway' terms (Fig. 4E). These findings suggested that POLQ could promote EC progression by enhancing DNA repair capacity and facilitating cell cycle progression.

POLQ promotes EC cell proliferation, migration, invasion and epithelial-mesenchymal transition (EMT) in vitro. To investigate the biological role of POLQ in EC *in vitro*, the HEC-1-B and Ishikawa cell lines were selected. Firstly, POLQ expression at both the mRNA and protein levels was assessed following cell transfection with si-NC, si-POLQ#1 or si-POLQ#2 for 48 h. The results showed that both si-POLQ#1 and si-POLQ#2 efficiently suppressed POLQ expression compared with that in the si-NC group (Fig. 5A and B). Functional assays demonstrated that POLQ

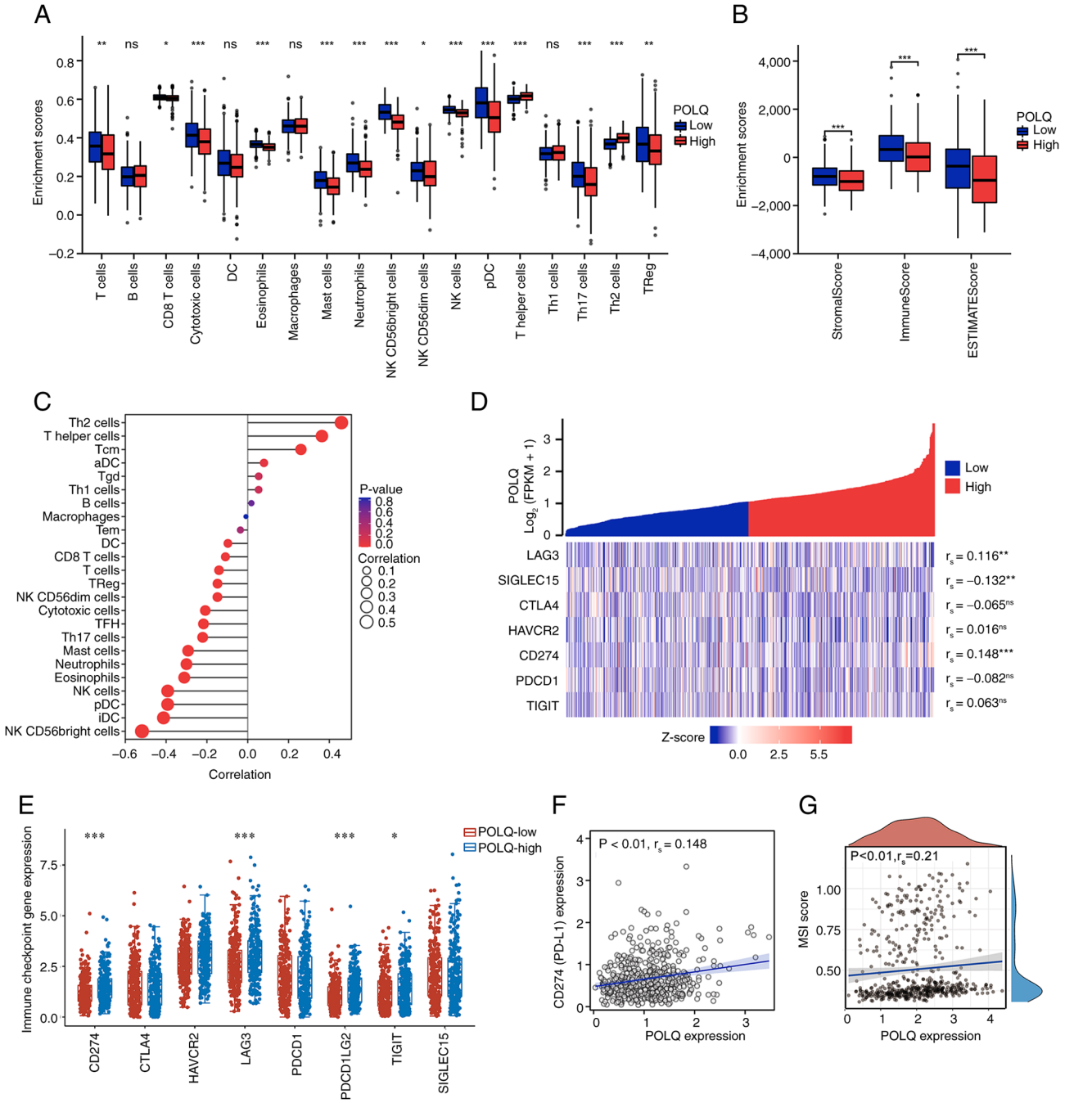

Figure 2. Immune infiltration analysis of POLQ in EC. (A) Immune cell abundance of high- or low-POLQ expression groups in EC. (B) Immune infiltration analyses of the ESTIMATE algorithm, including stromal score, immune score and ESTIMATE score in EC with high- and low-POLQ expression. (C) Correlation analyses of immune cells and POLQ expression. (D) Correlation analysis between immune checkpoint-related molecules and POLQ expression. (E) Expression levels of immune checkpoint-related genes in high- and low-POLQ expression groups. Correlation analysis (F) between CD274 (PD-L1) and POLQ expression, and (G) between MSI score and POLQ expression in EC. *P<0.05, **P<0.01, ***P<0.001. aDC, activated DC; DC, dendritic cell; EC, endometrial cancer; ESTIMATE, Estimation of Stromal and Immune Cells in Malignant Tumor Tissues using Expression Data; iDC, immature DC; MSI, microsatellite instability; NK, natural killer; ns, not significant; pDC, plasmacytoid DC; PD-L1, programmed death-ligand 1; POLQ, DNA polymerase θ; THF, T follicular helper; Th, T helper; TReg, regulatory T.

knockdown markedly inhibited HEC-1-B and Ishikawa cell proliferation, as evidenced by the CCK-8 assays (Fig. 5C) and reduced EdU incorporation (Fig. 5D). Consistently, colony formation ability was significantly reduced in POLQ-silenced cells (Fig. 5E). Transwell assays further revealed that POLQ knockdown notably impaired both the migratory and invasive capacities of HEC-1-B and Ishikawa cells (Fig. 5F), while wound healing assays confirmed a pronounced reduction in cell migration following POLQ silencing (Fig. 5G). At the molecular level, western blot analysis demonstrated that POLQ knockdown modulated the expression levels of EMT-related proteins, characterized by E-cadherin upregulation, and downregulation of N-cadherin and vimentin (Fig. 5H). These results suggested that POLQ could promote EC progression by facilitating EMT.

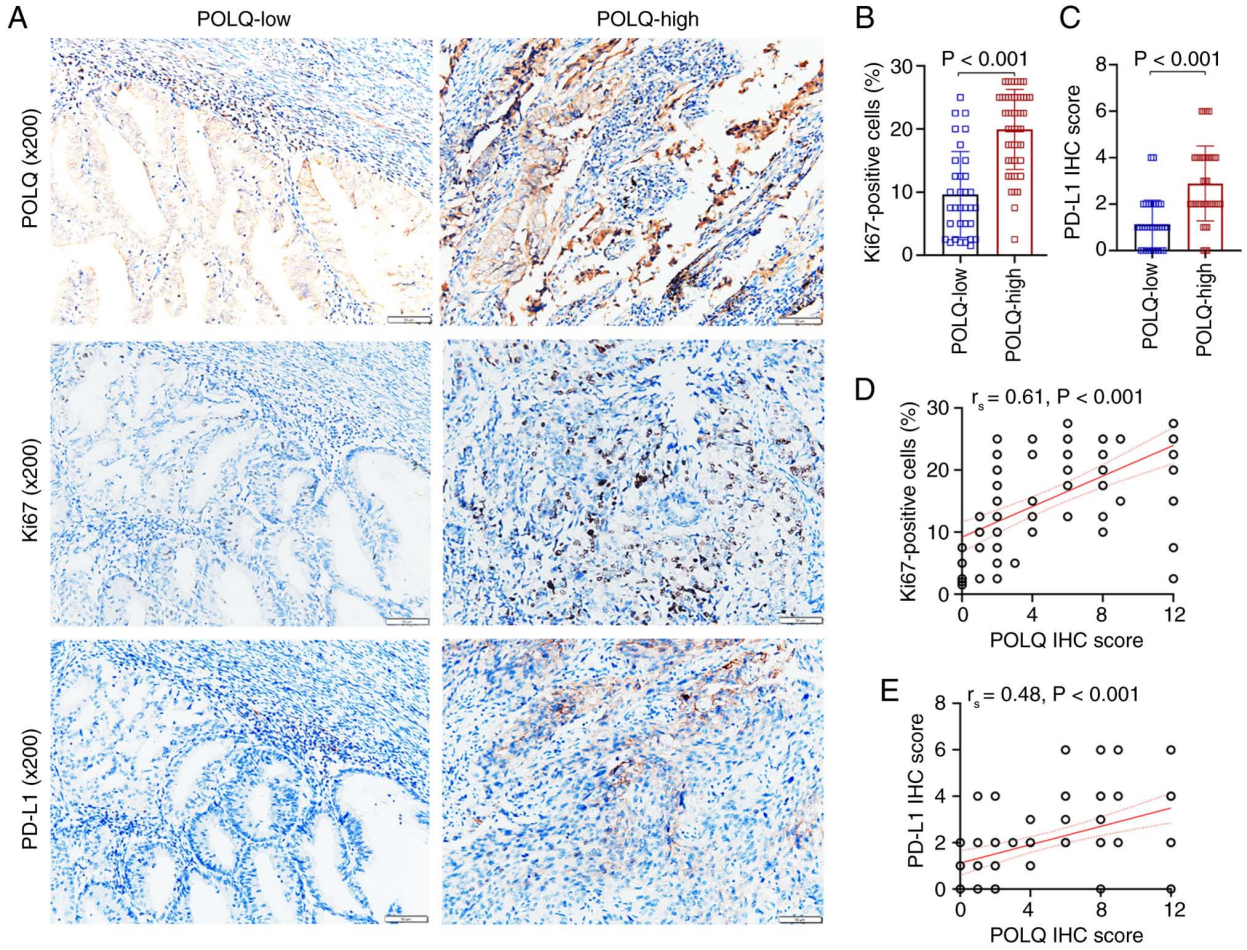

Figure 3. POLQ expression is positively correlated with Ki67 and PD-L1 expression. (A) IHC images of POLQ, Ki67, and PD-L1 expression in endometrial cancer; x200 magnification. Statistical analysis of (B) Ki67$^+$ cells and (C) PD-L1 IHC score in POLQ-high and -low expression groups. Correlation analysis between POLQ and (D) Ki67$^+$ cells or (E) PD-L1 IHC score. IHC, immunohistochemistry; PD-L1, programmed death-ligand 1; POLQ, DNA polymerase θ.

POLQ regulates apoptosis and cell cycle progression via the ataxia-telangiectasia mutated (ATM)/P53 pathway in EC cells. Flow cytometric analysis revealed that POLQ knockdown significantly promoted HEC-1-B and Ishikawa cell apoptosis compared with that in the si-NC group (Fig. 6A). In addition, POLQ silencing significantly altered cell cycle distribution, with a decreased proportion of cells in the G_2/M phase, indicating impaired cell cycle progression (Fig. 6B). Consistently, RT-qPCR analysis demonstrated that knockdown of POLQ markedly reduced the expression levels of key cell cycle-related regulators, including P21, cyclin-dependent kinase 1 (CDK1) and cyclin B1 (CCNB1) (Fig. 6C). At the protein level, western blot analysis confirmed that POLQ knockdown could markedly decrease the protein expression levels of phosphorylated (P)-P53, P21, CDK1, CCNB1, P-ATM and P-checkpoint kinase 2 (CHK2) in both HEC-1-B and Ishikawa cells (Fig. 6D). Collectively, these results indicated that POLQ could regulate cell cycle progression and apoptosis in EC cells by modulating the ATM-mediated P53 signaling pathway.

Discussion

EC is one of the most common gynecological malignancies, with a steadily increasing global incidence (25). Its pronounced histological and molecular heterogeneity is reflected by distinct genomic alterations, including TP53 and POLE mutations, as well as recurrent somatic copy number alterations such as HER-2 amplification (26,27). It has been reported that POLQ, a highly conserved DNA polymerase that mediates an alternative DSB repair pathway, known as POLQ-mediated end joining, is upregulated in several types of cancer, including gastric cancer, cervical cancer, pancreatic carcinoma, breast cancer and lung adenocarcinoma, thus conferring survival advantages to cancer cells and promoting tumor progression (10,12,14,16,28,29). The results of the present study revealed significant POLQ upregulation in EC tumors compared with in normal endometrial tissues, as evidenced by integrated bioinformatics analysis and validation in a human tissue cohort. These findings suggested that POLQ could represent a promising therapeutic strategy for inhibiting EC initiation and progression.

Tumor cells are frequently subjected to DNA damage, including DSBs and mutations, which should be efficiently repaired to maintain cellular function (30). POLQ serves a critical role in repairing such DNA injuries, thereby supporting tumor cell survival, continuous proliferation and resistance to cell death. Acting as a tumor promoter, POLQ can affect several cellular processes through distinct regulatory networks. For example, Yao *et al* (10) demonstrated that POLQ knockdown could inhibit cell cycle progression by suppressing the expression

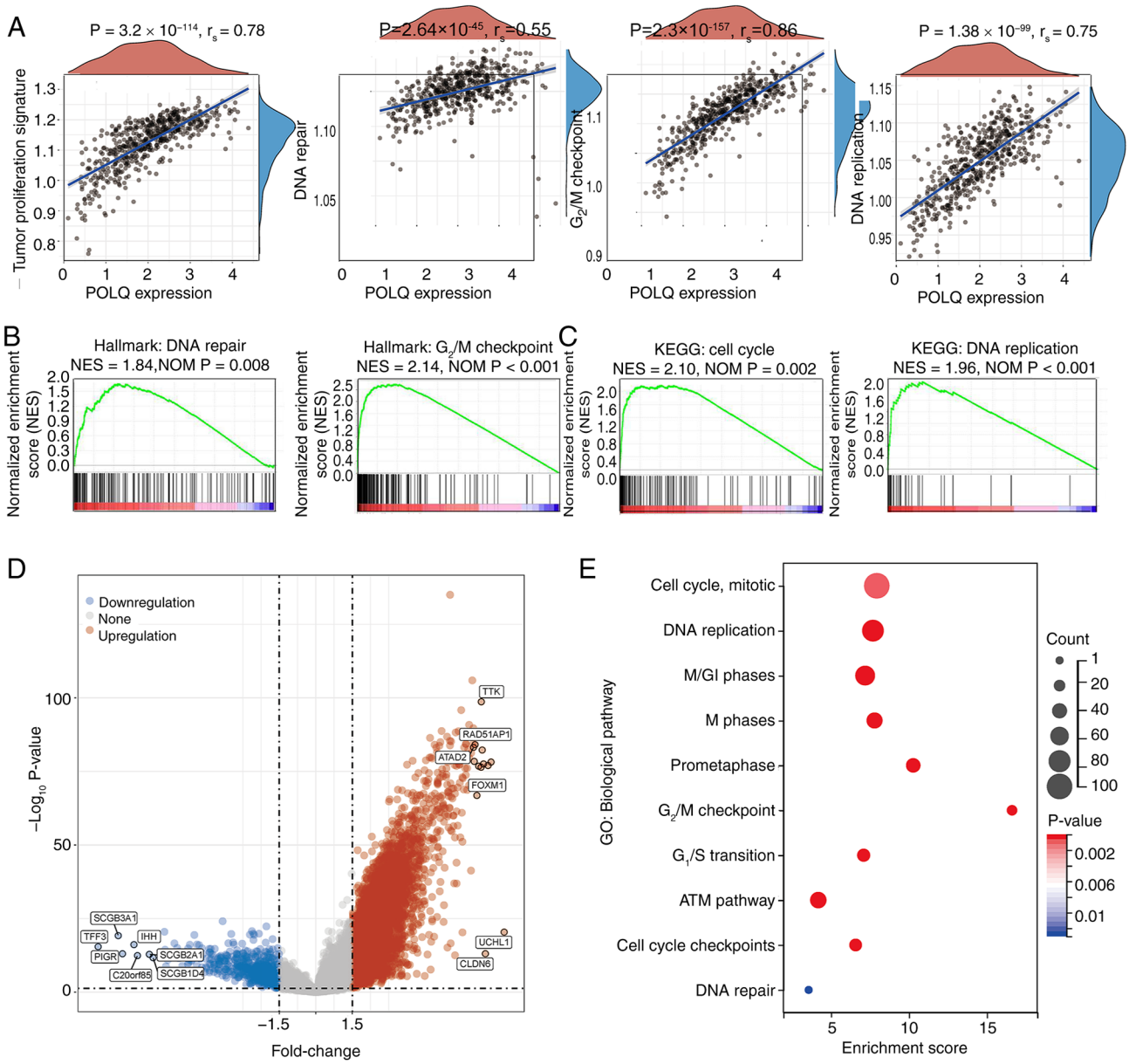

Figure 4. GSEA and functional enrichment analysis of POLQ in EC. (A) GSEA of POLQ-involved signaling pathways in EC. (B) The hallmark enrichment analysis and (C) KEGG functional enrichment analysis of the signaling pathways associated with high POLQ expression in EC. (D) Volcano plot of the differentially expressed genes in the POLQ-high and -low expression groups. (E) GO enrichment analysis of differentially expressed genes. EC, endometrial cancer; GO, Gene Ontology; GSEA, Gene Set Enrichment Analysis; KEGG, Kyoto Encyclopedia of Genes and Genomes; NES, normalized enrichment score; POLQ, DNA polymerase θ.

of proteins associated with the G_1/M and S/M phases of the cell cycle in colorectal cancer. In addition, Pan *et al* (31) reported that POLQ depletion could disrupt the progression of hepatocellular carcinoma by impairing cell proliferation, whereas Li *et al* (32) showed that POLQ silencing suppressed tumor growth via activation of the cyclic GMP/AMP synthase (cGAS)/stimulator of interferon genes (STING)/interferon-stimulated genes pathway in esophageal squamous cell carcinoma. Furthermore, POLQ has been reported to be involved in maintaining cancer stemness and conferring resistance to ferroptosis in gastric cancer cells (12). Collectively, the aforementioned studies from other malignancies suggest that POLQ upregulation may be associated with poor survival in EC, primarily via enhancing DNA repair capacity, sustaining replication and promoting G_2/M cell cycle progression.

Consistent with the aforementioned observations, the analysis of TCGA-EC cohort in the present study revealed a significant association between POLQ expression and clinicopathological features, including clinical stage and histological grade. Elevated POLQ expression was also significantly associated with worse OS and DSS, thus highlighting its potential prognostic value in EC. Consistently, POLQ expression was positively associated with $Ki67^+$ proliferation index, further supporting its role in promoting tumor cell proliferation. Functional experiments further verified that POLQ can enhance EC cell proliferation and progression. Nevertheless, the relatively limited sample size underscores the need for validation in larger cohorts, as well as *in vivo* studies and potential clinical trials to fully elucidate the therapeutic relevance of POLQ in EC.

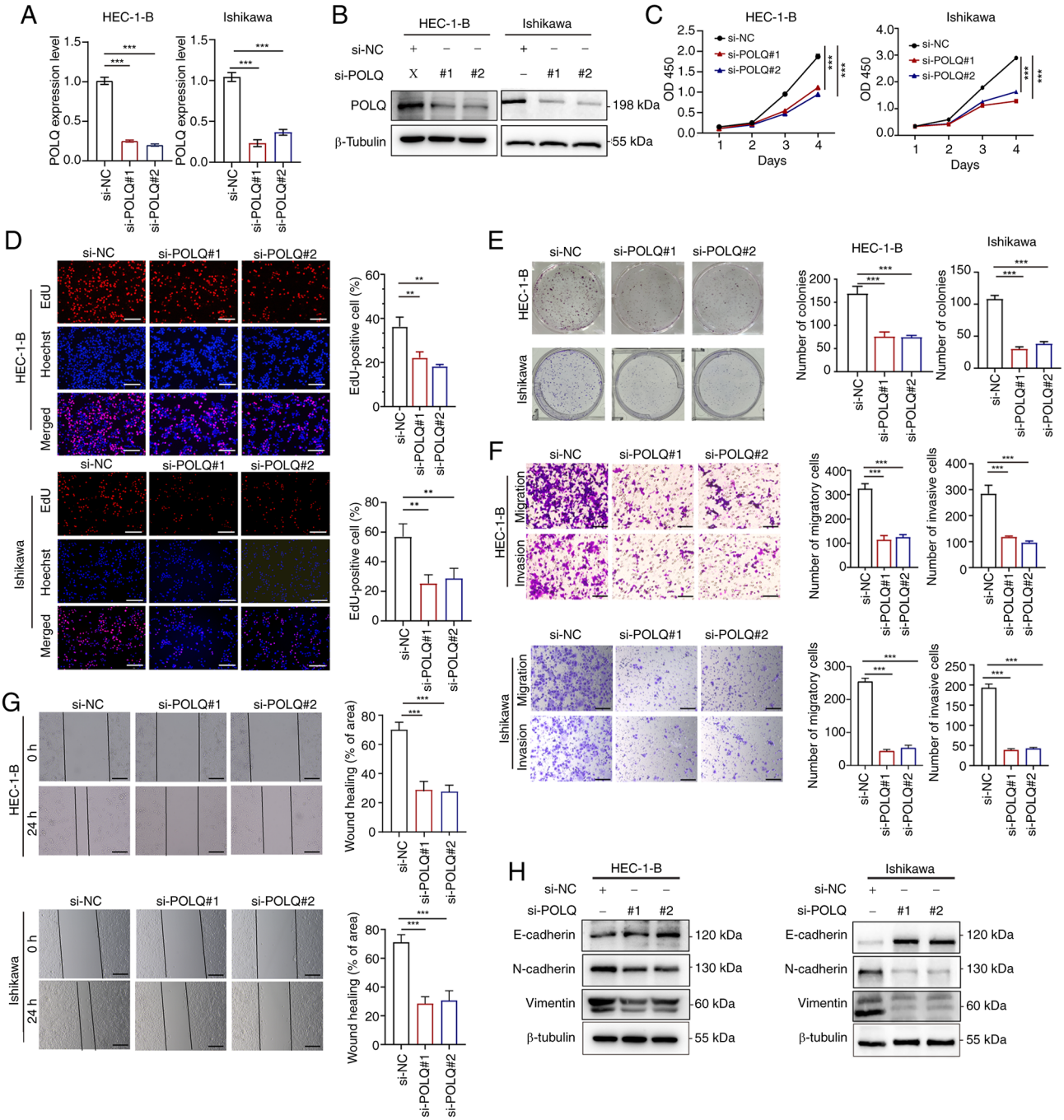

Figure 5. Aberrant POLQ expression affects cell proliferation and invasion in endometrial cancer cell lines. (A) mRNA and (B) protein expression levels of POLQ in HEC-1-B and Ishikawa cells transfected with si-NC, si-POLQ#1 and si-POLQ#2. Results of the (C) CCK-8 assay, (D) EdU experiment (scale bar, 50 μm), (E) colony formation assay, (F) Transwell assays (x10 magnification; scale bar, 200 μm) and (G) wound healing assay of transfected HEC-1-B and Ishikawa cells (x10 magnification; scale bar, 200 μm. (H) Western blotting of proteins related to epithelial-mesenchymal transition in HEC-1-B and Ishikawa cells transfected with si-NC, si-POLQ#1 and si-POLQ#2. For each cell line, western blot analyses were performed using samples derived from the same experimental panel and normalized to the same loading control antibody (β-tubulin). All experiments were performed in triplicate. **P<0.01, ***P<0.001. NC, negative control; POLQ, DNA polymerase θ; si, small interfering.

Tumor-immune homeostasis serves a critical role in tumor initiation and progression. Activation of the PD-L1 signaling pathway can enable tumor immune evasion, whereas its inhibition can enhance endogenous antitumor immunity (33). Notably, POLQ inhibition has been reported to activate the cGAS/STING pathway, thereby promoting immune cell infiltration (17,32). In bladder cancer, the combined assessment of POLQ and PD-L1 expression could serve as a predictor of immunotherapy efficacy (34), thus suggesting a role for POLQ in modulating the tumor microenvironment. In line with these findings, the present study revealed that high POLQ expression was associated with reduced immune and stromal scores, and diminished infiltration of antitumor immune cells, including $CD8^+$ T cells and NK cells. Furthermore, POLQ expression was positively correlated with PD-L1 levels in both TCGA dataset and validation cohort, although the correlation in the TCGA dataset was weak, suggesting a potential association between POLQ and the immunosuppressive

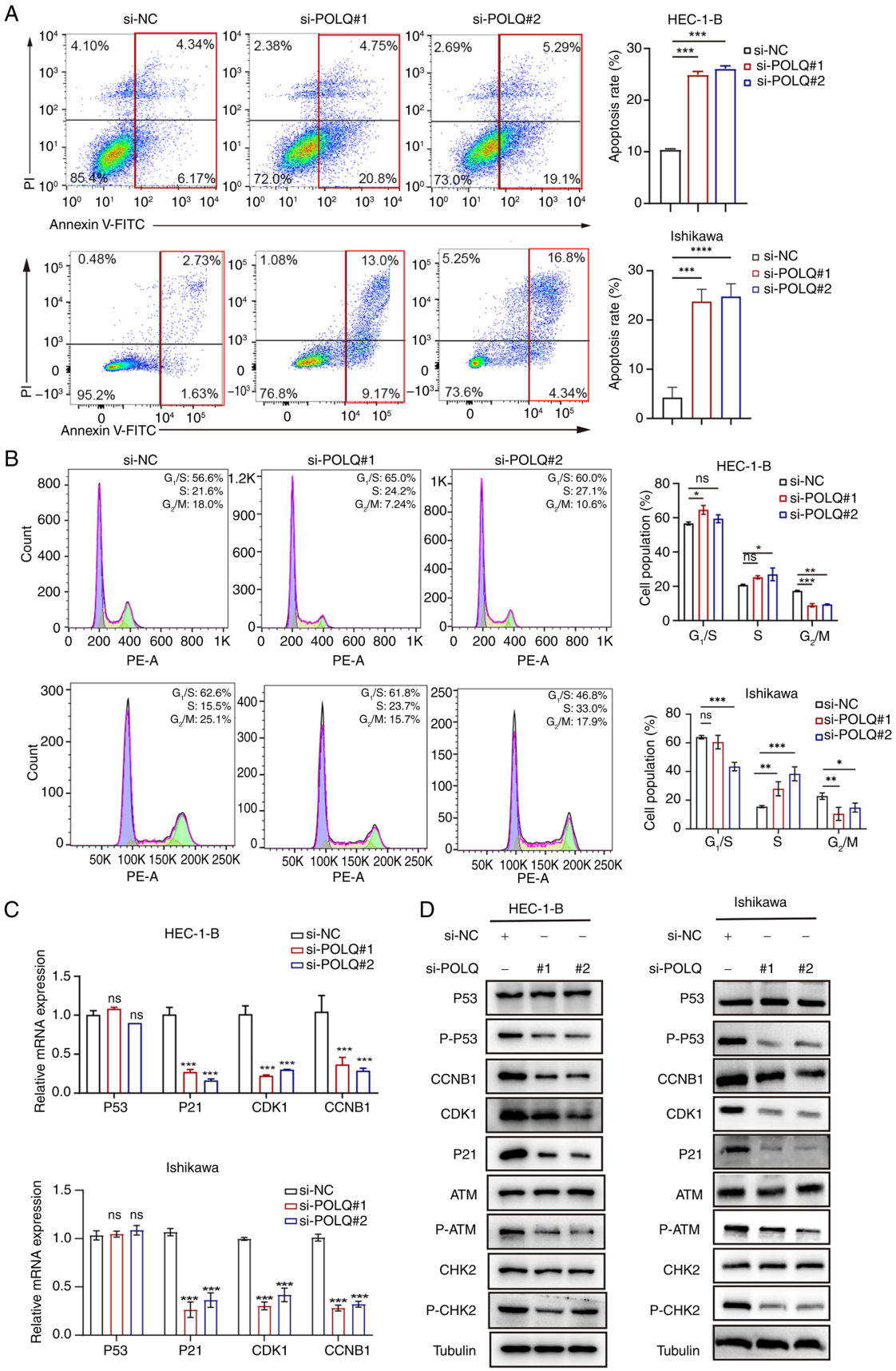

Figure 6. Silencing POLQ promotes apoptosis, induces S-phase accumulation with a decreased proportion of cells in the G_2/M-phase, and attenuates ATM-CHK2-mediated DNA damage response signaling in endometrial cancer cell lines. (A) Apoptosis analysis and (B) cell cycle analysis of HEC-1-B and Ishikawa cells transfected with si-NC, si-POLQ#1 and si-POLQ#2. (C) mRNA and (D) protein expression levels of G_2/M-related genes and the ATM signaling pathway in HEC-1-B and Ishikawa cells. For each cell line, western blot analyses were performed using samples derived from the same experimental panel and normalized to the same loading control antibody (β-tubulin). All experiments were performed in triplicate. *P<0.05, **P<0.01, ***P<0.001, ****P<0.0001vs. si-NC or as indicated. ATM, ataxia-telangiectasia mutated; CCNB1, cyclin B1; CDK1, cyclin-dependent kinase 1; CHK2, checkpoint kinase 2; NC, negative control; ns, not significant; P-, phosphorylated; PI, propidium iodide; POLQ, DNA polymerase θ; si, small interfering.

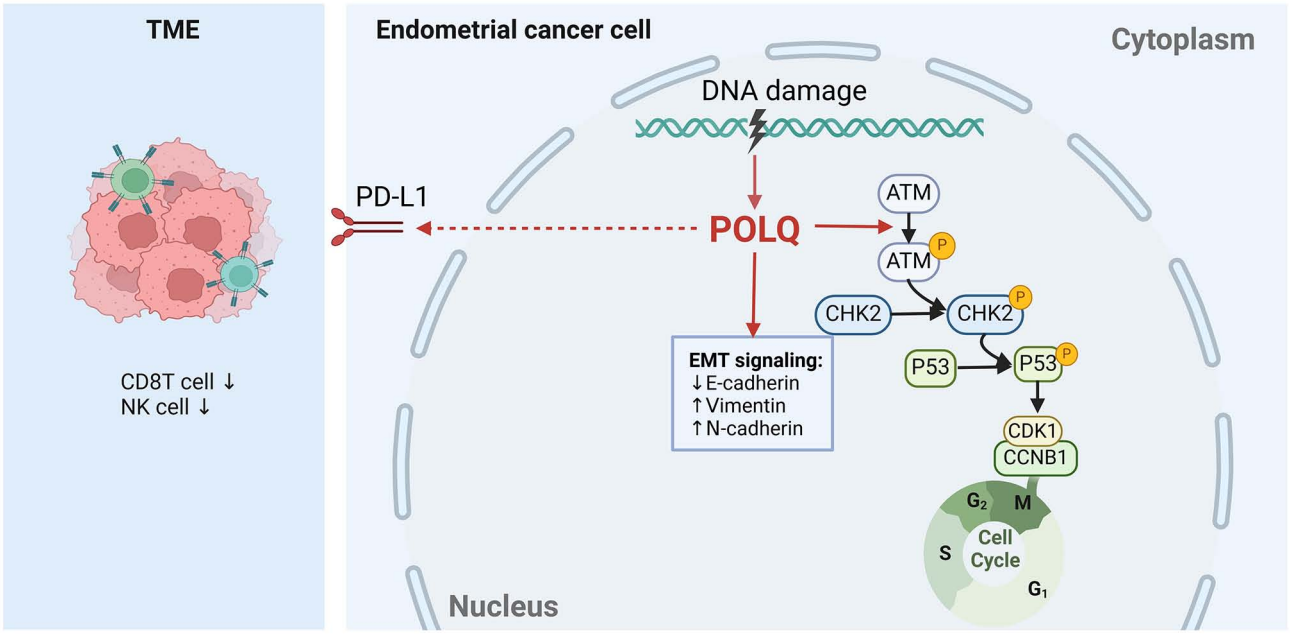

Figure 7. Schematic diagram. POLQ is upregulated in EC and drives tumor progression by activating ATM/P53 signaling, inducing EMT through cadherin switching, and promoting an immunosuppressive microenvironment via PD-L1 upregulation. POLQ upregulation is associated with aggressive clinicopathological features in EC, indicating its potential as a prognostic biomarker and therapeutic target. ATM, ataxia-telangiectasia mutated; CCNB1, cyclin B1; CDK1, cyclin-dependent kinase 1; CHK2, checkpoint kinase 2; EMT, epithelial-mesenchymal transition; NK, natural killer; PD-L1, programmed death-ligand 1; POLQ, DNA polymerase θ; TME, tumor microenvironment.

tumor microenvironment in EC. The present study primarily focused on characterizing the immunosuppressive landscape associated with POLQ expression, with particular attention to PD-L1 expression and the infiltration of T cells and NK cells. Although these analyses provide initial insights into the potential immunoregulatory role of POLQ, a comprehensive evaluation of immunotherapy response and additional immune cell subtypes was beyond the scope of the current work. Therefore, further studies incorporating functional assays, broader immune profiling and immunotherapy-related models will be required to fully elucidate the role of POLQ in tumor immune regulation.

GSEA indicated that POLQ was primarily involved in cell cycle regulation, DNA repair and DNA replication, consistent with its key role in the DNA damage response (DDR). Previous studies have suggested that POLQ inhibitors enhance radiosensitivity in human colorectal cancer (HCT116), non-small cell lung cancer (H460) and bladder cancer (T24) cell lines, as well as in mouse xenograft models in preclinical settings (35) , highlighting its pivotal function in DNA repair. DNA damage commonly arising from metabolic processes and environmental factors can activate DDR mechanisms designated to maintain genomic stability (36). In the current study, POLQ expression was associated with the ATM signaling pathway, a key regulator of multiple DDR cascades. Upon the occurrence of DSBs, ATM is activated through autophosphorylation at Ser1981 (37). *In vitro* experiments demonstrated that POLQ knockdown inhibited EC cell proliferation, invasion and metastasis. Mechanistically, POLQ depletion reduced the phosphorylation of ATM and CHK2, suggesting impaired activation of the DNA damage response pathway, which may subsequently influence downstream signaling pathways, including the P53 signaling pathway and its downstream effectors, such as P21, CDK1 and CCNB1. Consequently, POLQ inhibition altered cell cycle distribution, characterized by a reduced proportion of cells in the G_2/M phase, and promoted apoptosis.

Synthetic lethality represents a key strategy in anticancer drug development. Preclinical studies have shown that POLQ inhibitors can act synergistically with poly(ADP-ribose) polymerase (PARP) inhibitors to overcome resistance to PARP-targeted therapies (9,38). Recently, POLQ-targeting compounds, including novobiocin, have been identified as potential anticancer agents (39). Therefore, investigating the role of POLQ in EC could provide novel insights into the development of efficient synthetic lethal therapies, thus offering novel therapeutic strategies for patients with EC.

Collectively, the current study provided a comprehensive analysis of POLQ upregulation in EC, demonstrating its association with poor prognosis based on multiple public databases and clinical specimens. POLQ expression was positively correlated with Ki67 and PD-L1, thus supporting its involvement in tumor cell proliferation and immunosuppression. *In vitro* experiments further showed that POLQ could facilitate G_2/M-phase cell cycle progression, activate the ATM-mediated P53 signaling pathway and promote EMT in EC cells, as summarized in Fig. 7. Taken together, these findings highlighted POLQ and its associated pathways as potential prognostic biomarkers and therapeutic targets in EC. Although elevated POLQ expression was associated with a poor prognosis, multivariate Cox regression analysis indicated that POLQ was not an independent prognostic factor. This represents an important limitation of the present study, suggesting that POLQ alone may not be sufficient as a standalone prognostic biomarker and may instead function as part of a broader regulatory network. Future studies incorporating

larger, independent cohorts, integrated biomarker analyses and mechanistic investigations will be required to further define the prognostic relevance of POLQ. In addition, prospective studies are needed to assess whether POLQ may have clinical value in combination with other established prognostic factors.

Acknowledgments

The authors would like to thank Dr Hanmao Tong and Dr Xianbin Tang (Department of Pediatrics, Affiliated Taihe Hospital of Hubei University of Medicine, Shiyan, Hubei, China) for their administrative support in facilitating the ethics approval process.

Funding

The present study was supported by the Bethune Charity Foundation (grant no. 4-1-281).

Availability of data and materials

The data generated in the present study may be requested from the corresponding author.

Authors' contributions

NZ developed the bioinformatics analysis strategy, performed the experiments and conducted the statistical analyses. NZ, JW and XZ performed formal analysis and investigation. NZ and JW prepared the original draft. NZ, JW and XZ reviewed and edited the manuscript. YH acquired funding, contributed to the study conception and critically revised the manuscript. LG was responsible for providing key experimental materials and technical resources, and contributed to data acquisition and interpretation. KT supervised the study, contributed to the experimental design and interpretation of the data, and critically revised the manuscript. NZ and JW confirm the authenticity of all the raw data. All authors contributed to the experiments, and read and approved the final manuscript.

Ethics approval and consent to participate

The present study was approved by the Ethics Committee of Affiliated Taihe Hospital of Hubei University of Medicine (approval no. 2023KS58; Shiyan, China). All procedures involving human participants were conducted in accordance with The Declaration of Helsinki. Written informed consent for the use of residual pathological specimens for this research and future related studies was obtained from all patients. All samples were rigorously de-identified.

Patient consent for publication

Not applicable.

Competing interests

The authors declare that they have no competing interests.

References

1. Siegel RL, Giaquinto AN and Jemal A: Cancer statistics, 2024. CA Cancer J Clin 74: 12-49, 2024.
2. Makker V, MacKay H, Ray-Coquard I, Levine DA, Westin SN, Aoki D and Oaknin A: Endometrial cancer. Nat Rev Dis Primers 7: 88, 2021.
3. van den Heerik A, Horeweg N, de Boer SM, Bosse T and Creutzberg CL: Adjuvant therapy for endometrial cancer in the era of molecular classification: radiotherapy, chemoradiation and novel targets for therapy. Int J Gynecol Cancer 31: 594-604, 2021.
4. Wood RD and Doublié S: DNA polymerase θ (POLQ), double-strand break repair, and cancer. DNA Repair (Amst) 44: 22-32, 2016.
5. Yousefzadeh MJ, Wyatt DW, Takata K, Mu Y, Hensley SC, Tomida J, Bylund GO, Doublié S, Johansson E, Ramsden DA, *et al*: Mechanism of suppression of chromosomal instability by DNA polymerase POLQ. PLoS Genet 10: e1004654, 2014.
6. Seki M, Masutani C, Yang LW, Schuffert A, Iwai S, Bahar I and Wood RD: High-efficiency bypass of DNA damage by human DNA polymerase Q. EMBO J 23: 4484-4494, 2004.
7. Ceccaldi R, Liu JC, Amunugama R, Hajdu I, Primack B, Petalcorin MI, O'Connor KW, Konstantinopoulos PA, Elledge SJ, Boulton SJ, *et al*: Homologous-recombination-deficient tumours are dependent on Polθ-mediated repair. Nature 518: 258-262, 2015.
8. Mateos-Gomez PA, Gong F, Nair N, Miller KM, Lazzerini-Denchi E and Sfeir A: Mammalian polymerase θ promotes alternative NHEJ and suppresses recombination. Nature 518: 254-257, 2015.
9. Zatreanu D, Robinson HMR, Alkhatib O, Boursier M, Finch H, Geo L, Grande D, Grinkevich V, Heald RA, Langdon S, *et al*: Polθ inhibitors elicit BRCA-gene synthetic lethality and target PARP inhibitor resistance. Nature Commun 12: 3636, 2021.
10. Yao Q, Gao S, Sun Q, Liuhua W, Ren J and Wang D: POLQ knockdown inhibits proliferation, migration, and invasion by inducing cell cycle arrest in colorectal cancer. Discov Oncol 15: 633, 2024.
11. Shinmura K, Kato H, Kawanishi Y, Yoshimura K, Tsuchiya K, Takahara Y, Hosokawa S, Kawase A, Funai K and Sugimura H: POLQ Overexpression Is associated with an increased somatic mutation load and PLK4 overexpression in lung adenocarcinoma. Cancers (Basel) 11: 722, 2019.
12. Peng Y, Zheng W, Chen Y, Lei X, Yang Z, Yang Y, Liang W, Sun K, Li G and Yu J: POLQ inhibition attenuates the stemness and ferroptosis resistance in gastric cancer cells via downregulation of dihydroorotate dehydrogenase. Cell Death Dis 15: 248, 2024.
13. Kunihisa T, Inubushi S, Tanino H and Hoffman RM: Induction of the DNA-repair gene POLQ only in BRCA1-mutant breast-cancer cells by methionine restriction. Cancer Genomics Proteomics 21: 399-404, 2024.
14. Zang Y, Zhao R, Wang T, Gao Y, Chen L, Liu S, Wang Y and Xue F: Identification of *POLQ* as a key gene in cervical cancer progression using integrated bioinformatics analysis and experimental validation. Mol Med Rep 27: 115, 2023.
15. Patterson-Fortin J and D'Andrea AD: Targeting polymerase theta (POLθ) for cancer therapy. Cancer Treat Res 186: 285-298, 2023.
16. Del Puerto-Nevado L, Fernández-Aceñero MJ, Cebrián A, Fatych Y, Díez-Valladares LI, Pérez-Aguirre E, de la Serna S, García-Botella A, Martínez-Useros J, García-Foncillas J and Mateos-Gómez PA: POLQ immunostaining behaves as a prognostic factor for pancreatic carcinoma. Front Oncol 14: 1433179, 2024.
17. Oh G, Wang A, Wang L, Li J, Werba G, Weissinger D, Zhao E, Dhara S, Hernandez RE, Ackermann A, *et al*: POLQ inhibition elicits an immune response in homologous recombination-deficient pancreatic adenocarcinoma via cGAS/STING signaling. J Clin Invest 133: e165934, 2023.
18. Bartha Á and Győrffy B: TNMplot.com: A web tool for the comparison of gene expression in normal, tumor and metastatic tissues. Int J Mol Sci 22: 2622, 2021.
19. Yoshihara K, Shahmoradgoli M, Martínez E, Vegesna R, Kim H, Torres-Garcia W, Treviño V, Shen H, Laird PW, Levine DA, *et al*: Inferring tumour purity and stromal and immune cell admixture from expression data. Nat Commun 4: 2612, 2013.
20. Hänzelmann S, Castelo R and Guinney J: GSVA: Gene set variation analysis for microarray and RNA-seq data. BMC Bioinformatics 14: 7, 2013.

21. Huber W, Carey VJ, Gentleman R, Anders S, Carlson M, Carvalho BS, Bravo HC, Davis S, Gatto L, Girke T, *et al*: Orchestrating high-throughput genomic analysis with bioconductor. Nat Methods 12: 115-121, 2015.
22. Subramanian A, Tamayo P, Mootha VK, Mukherjee S, Ebert BL, Gillette MA, Paulovich A, Pomeroy SL, Golub TR, Lander ES and Mesirov JP: Gene set enrichment analysis: A knowledge-based approach for interpreting genome-wide expression profiles. Proc Natl Acad Sci U S A 102: 15545-15550, 2005.
23. Pasanen A, Loukovaara M and Bützow R: Clinicopathological significance of deficient DNA mismatch repair and MLH1 promoter methylation in endometrioid endometrial carcinoma. Mod Pathol 33: 1443-1452, 2020.
24. Livak KJ and Schmittgen TD: Analysis of relative gene expression data using real-time quantitative PCR and the 2-ΔΔCT method. Methods 25: 402-408, 2001.
25. Crosbie EJ, Kitson SJ, McAlpine JN, Mukhopadhyay A, Powell ME and Singh N: Endometrial cancer. Lancet 399: 1412-1428, 2022.
26. Huvila J, Pors J, Thompson EF and Gilks CB: Endometrial carcinoma: Molecular subtypes, precursors and the role of pathology in early diagnosis. J Pathol 253: 355-365, 2021.
27. Urick ME and Bell DW: Clinical actionability of molecular targets in endometrial cancer. Nat Rev Cancer 19: 510-521, 2019.
28. Higgins GS, Harris AL, Prevo R, Helleday T, McKenna WG and Buffa FM: Overexpression of POLQ confers a poor prognosis in early breast cancer patients. Oncotarget 1: 175-184, 2010.
29. Rao X, Xing B, Wu Z, Bin Y, Chen Y, Xu Y, Zhou D, Zhou X, Wu C, Ye W, *et al*: Targeting polymerase θ impairs tumorigenesis and enhances radiosensitivity in lung adenocarcinoma. Cancer Sci 114: 1943-1957, 2023.
30. Hanahan D: Hallmarks of Cancer: New dimensions. Cancer Discov 12: 31-46, 2022.
31. Pan Q, Wang L, Liu Y, Li M, Zhang Y, Peng W, Deng T, Peng ML, Jiang JQ, Tang J, *et al*: Knockdown of POLQ interferes the development and progression of hepatocellular carcinoma through regulating cell proliferation, apoptosis and migration. Cancer Cell Int 21: 482, 2021.
32. Li J, Ko JM, Dai W, Yu VZ, Ng HY, Hoffmann JS and Lung ML: Depletion of DNA polymerase theta inhibits tumor growth and promotes genome instability through the cGAS-STING-ISG pathway in esophageal squamous cell carcinoma. Cancers (Basel) 13: 3204, 2021.
33. Kornepati AVR, Vadlamudi RK and Curiel TJ: Programmed death ligand 1 signals in cancer cells. Nat Rev Cancer 22: 174-189, 2022.
34. Liu G, Jin K, Liu Z, Su X, Xu Z, Li B, Xu J, Chang Y, Wang Y, Zhu Y, *et al*: POLQ identifies a better response subset to immunotherapy in muscle-invasive bladder cancer with high PD-L1. Cancer Med 13: e6962, 2024.
35. Checcucci E, Bignante G, Volpi G, Liguori S, Alessio P, Sica M, Ortenzi M, Amparore D, Saliva A, Piana A, *et al*: Small-molecule Polθ inhibitors provide safe and effective tumor radiosensitization in preclinical models. Clin Cancer Res 29: 1631-1642, 2023.
36. Chatterjee N and Walker GC: Mechanisms of DNA damage, repair, and mutagenesis. Environ Mol Mutagen 58: 235-263, 2017.
37. Jin MH and Oh DY: ATM in DNA repair in cancer. Pharmacol Ther 203: 107391, 2019.
38. Seed G, Beije N, Yuan W, Bertan C, Goodall J, Lundberg A, Tyler M, Figueiredo I, Pereira R, Baker C, *et al*: Elucidating acquired PARP inhibitor resistance in advanced prostate cancer. Cancer Cell 42: 2113-2123.e2114, 2024.
39. Syed A, Filandr F, Patterson-Fortin J, Bacolla A, Ravindranathan R, Zhou J, McDonald DT, Albuhluli ME, Verway-Cohen A, Newman JA, *et al*: Novobiocin blocks nucleic acid binding to Polθ and inhibits stimulation of its ATPase activity. Nucleic Acids Res 51: 9920-9937, 2023.